

## RESEARCH ARTICLE

# Compact Patch Antenna Array With Fan-Beam Characteristics for Radar Application

SEYED HOJATOLLAH MADANI<sup>1</sup>, YASHAR ZEHFOROOSH<sup>2</sup>, AND TOHID SEDGHI<sup>2</sup><sup>1</sup>Department of Electrical Engineering, Islamic Azad University, Urmia Branch, Urmia 63896-57169, Iran<sup>2</sup>Microwave and Antenna Research Center, Islamic Azad University, Urmia Branch, Urmia 63896-57169, Iran

Corresponding author: Yashar Zehforoosh (y.zehforoosh@srbiau.ac.ir)

**ABSTRACT** In this paper, a compact  $1 \times 4$  patch array antenna with a fan-beam radiation pattern is introduced for use in 3.5 GHz band applications. The proposed antenna consists of a planar two-layer printed structure so that the radiation elements and feeding network are located in the upper and lower layers respectively. In this way, the antenna has very compact dimensions while achieving a high radiation gain. Using a reflector plane under the antenna has improved the radiation pattern and decreased the antenna back radiation. The fabricated array antenna has an impedance bandwidth of 3.35-3.75 GHz (11.27%), a maximum realized gain of 10.91 dBi, and half power beamwidths (HPBW) of  $23.86^\circ$  and  $85.44^\circ$  on the H- and E-panels, respectively. The overall dimensions of the antenna are  $209 \times 32.3 \times 3.708 \text{ mm}^3$  with a  $250 \times 50 \text{ mm}^2$  conductive reflector at a distance of  $\lambda/4$  from the antenna, and the theoretical and practical results show a good agreement with each other. The presented antenna is suitable for 5G systems and radar applications in the 3.5 GHz frequency band.


**INDEX TERMS** Antenna array, fan-beam pattern, radar, 5G system.

## I. INTRODUCTION

A fan-beam antenna is a directional antenna generating a narrow beamwidth in one plane and a wider beamwidth in the orthogonal plane [1]. Consequently, the surrounding space on one plane can be scanned. Generally, this type of pattern is accomplished using a truncated parabolic reflector or a circular paraboloid reflector by illuminating an asymmetrical section of the paraboloid [2]. Fan-beam antennas have many applications in the telecommunication systems, such as imaging [3], [4], radar systems [5], [6], [7], [8], beam steering [9], 5G components [10], [11], [12], industrial, scientific and medical (ISM) purposes [13], traffic monitoring [14], application of Photonic Bandgap (PBG) structures [15], Wireless Gigabit (WiGig) applications [16], back-haul antennas [17] and IEEE 802.11ac applications [18]. This type of antenna is mainly used in point-to-multipoint data transmission systems. Different techniques are employed to produce a fan-beam radiation pattern for the antenna. The use of Leaky-wave structures is one of the methods of forming

fan-beam radiation patterns [9], [15], [16]. In [9], a planar leaky-wave antenna is reported, which uses the Substrate Integrated Waveguide (SIW) structures in the antenna configuration to create the desired radiation pattern and is suitable for beam steering applications with compact dimensions. In addition, metasurface-based structures are good choices for this purpose [17], [19]. A planar structure of a metasurface lens is applied to create a narrow radiation pattern at a frequency of 10.4 GHz in [17]. Also, a radially gradient hybrid metasurface (RGHMS) is proposed in [19] fed by a slot antenna and achieves a narrow radiation pattern in the elevation plane for satellite communication. Using array structures is one of the most widely used methods for producing fan-beam radiation patterns [6], [8], [10], [11], [14], [18]. The presented array antennas in [6], [8], and [11] have eight elements, in [18] has ten elements, in [10] sixteen elements, and in [14] only two elements. All of the mentioned antennas use a fed network to excite the antenna elements. Subsequently, the use of the fed network increases the dimensions of the antenna and complicates its structure.

Recently, a compact 8-element array antenna with a fan-beam pattern for 5G applications is introduced [20].

The associate editor coordinating the review of this manuscript and approving it for publication was Ravi Kumar Gangwar .

An Artificial Magnetic Conductor (AMC) reflector is used in this work, is placed behind the array antenna elements, and creates a complex structure for the antenna. This antenna has a multi-layer structure, which uses two layers of substrates for its construction. The foremost advantages of multi-layer antennas are lower dielectric loss, compact dimension, facilitating the connection of the mounting surfaces with devices, and integrated circuits [21], [22].

A patch array antenna using four radiation elements is introduced in this work. A feeding network including Wilkinson power dividers is located in the lower layer of the antenna to feed the antenna elements. The two-layer structure reduces the dimensions of the antenna, and the input signal is transmitted to the antenna array elements over a shorter distance through four feeding pins. The results show that this antenna has a narrow radiation pattern in the  $zy$ - plane.

## II. WIDEBAND ANTENNA DESIGN WITH HIGH GAIN AT 3.5 GHz FREQUENCY

In the first step of the presented design in this paper, a planar printed antenna with coaxial feed is introduced. According to Fig. 1, the designed antenna is a patch antenna and consists of a bow-tie-shaped radiating element with a rectangular slot, in which a microstrip line is responsible for transmitting the signal from the coaxial cable to the radiation patch. This antenna is accomplished on an FR4 substrate with a thickness of 3.2 mm, a relative permittivity ( $\epsilon_r$ ) of 4.4, loss tangent ( $\tan \delta$ ) of 0.02, and an overall dimension of  $30 \times 50 \text{ mm}^2$ .

A complete conductor plate behind the radiation patch forms the ground plane of the antenna. The used excitation in the form of coaxial cable, allows the antenna to be easily fed by the conductor pin if the array structure is formed, with the fed network in the lower layer. Fig. 2 shows a comparison between the experimental results and the simulation of the return loss of the patch antenna. Both graphs show almost the same results. According to the simulated result, the designed patch antenna has an operating frequency band of 3.36-3.79 GHz (12.03%). However, the experiment shows that the antenna has an operating frequency band of 3.41-3.75 GHz (9.49%).

The  $L_s$  specifies the length of the rectangular-shaped slot of the patch. The length of the  $L_s$  parameter can change the position of the antenna resonance frequency and its bandwidth, as shown in Fig. 3. The figure indicates how the position of the center frequency decreases from 3.6 to 3.4 GHz by providing an increase in the length of the rectangular-shaped slot from 2 to 7 mm. Increasing the length of this slot can also diminish the antenna bandwidth. In this design, to achieve resonance at the frequency of 3.5 GHz, the length of the  $L_s$  is set at 5 mm.

The antenna radiation pattern is shown in Fig. 4. The patterns are relatively stable, and the Cross-polarization level is lower than the Co-polarization.

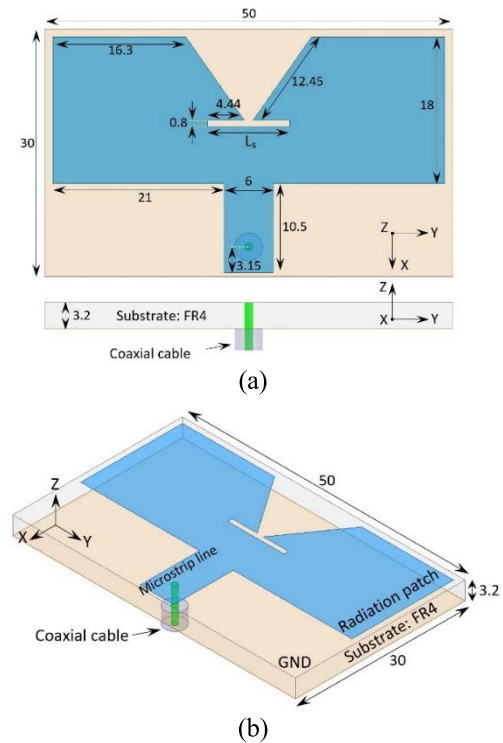


**FIGURE 1. Presentation of the patch antenna configuration (a) Dimensions of the patch antenna at the front and side views, and (b) 3D view and dimensions of the patch antenna.**

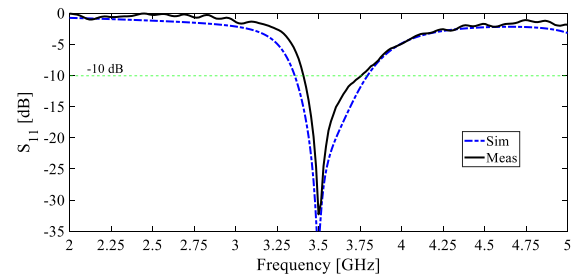


**FIGURE 2. Numerical and experimental impedance bandwidth of the patch antenna.**

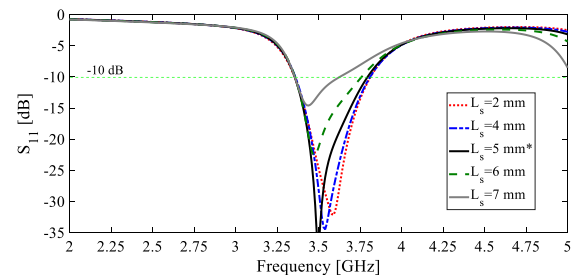


**FIGURE 3. The  $L_s$  parameter controls the bandwidth and the resonance frequency of the patch antenna.**

The numerical and experimental results related to the gain of the patch antenna are shown in Fig. 5. For this antenna, the maximum measured gain at the frequency of 3.5 GHz

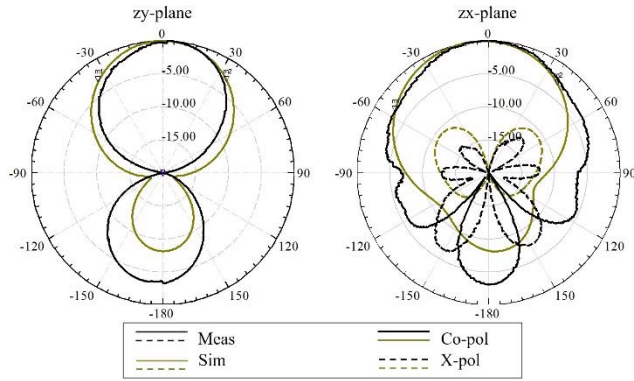


FIGURE 4. The radiation pattern of the patch antenna at 3.5 GHz.

equal to 4.38 dB has been reported. According to the results obtained from the proposed patch antenna, this design has a wide impedance bandwidth, high gain, and a stable radiation pattern. These results are achieved while the antenna has compact dimensions.

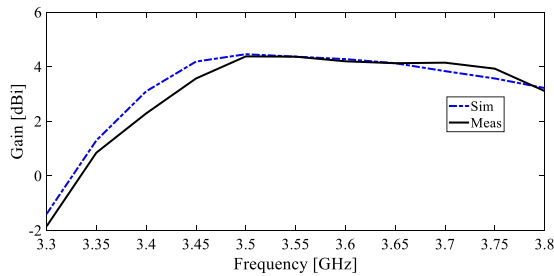


FIGURE 5. Simulated and measured gains of the patch antenna.

### III. THE FEEDING NETWORK

Four radiation elements are considered in this work. To feed the elements, a fed network is needed to excite them. For the fed network, two essential conditions are considered, 1. having compact dimensions and 2. having signal transmission to the elements with low losses. For this purpose, Wilkinson power dividers are used on the Rogers RO4003 substrate with a relative permittivity ( $\epsilon_r$ ) of 3.55 and a thickness of 0.508 mm. Fig. 6 (a) shows the Wilkinson power divider structure for power transmission and distribution in the 3.5 GHz frequency band. In addition, the simulation results related to this power divider are shown in Fig. 6 (b) and (c). The results show that using the Wilkinson structure on the Rogers substrate with a loss tangent ( $\tan \delta$ ) of 0.002 distributes the power evenly with very little loss and a negligible phase difference between the two output ports.

Using the proposed power divider structure, a feeding network is designed with four outputs, according to Fig. 7 (a). Furthermore, the feeding network simulation results are also shown in Fig. 7 (b) and (c). According to the results, we can see that the power transfer from the input to the outputs

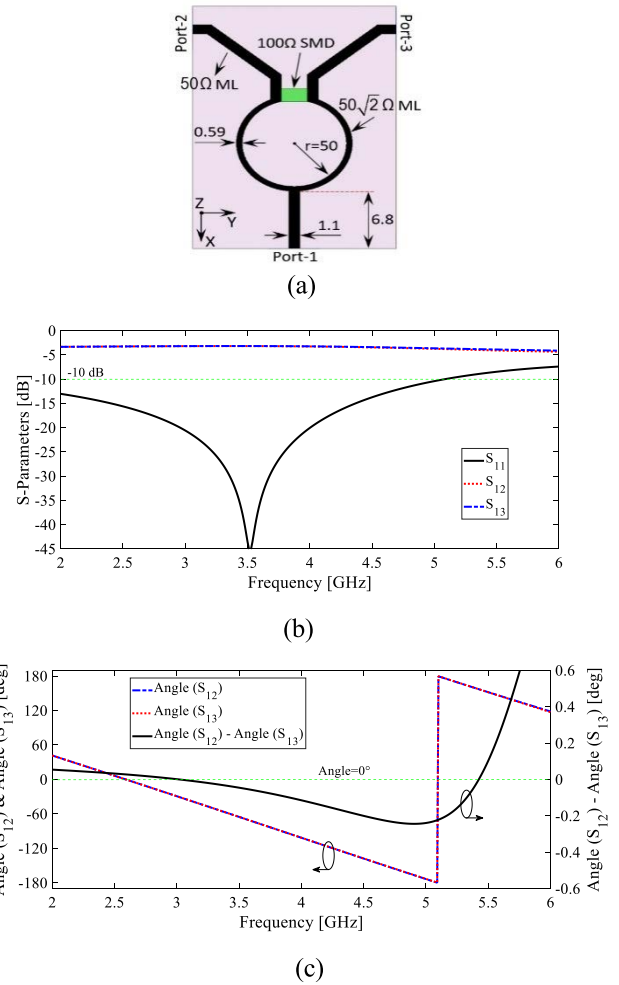


FIGURE 6. Configuration of the divider and simulations (a) dimensions of the proposed Wilkinson power divider, (b) S-parameters of the Wilkinson power divider, and (c) phase responses of the Wilkinson power divider(c).

of the feeding network with an insertion loss of about 0.6 dB ( $S_{1j} \approx -6.6$  dB), and we can ignore the phase difference between the output signals.

### IV. ANTENNA ARRAY WITH A FAN-BEAM RADIATION PATTERN

As discussed in Section II, the presented planar patch antenna in this work, similar to other patch antennas, has an average gain of approximately 4 dB and an HPBW of almost  $95.1^\circ$  and  $70.4^\circ$  on the E- and H-planes, respectively. These results are not sufficient for radar applications and 5G networks. According to [6] and [23], the directivity of the planar patch antenna can be approximated as follows:

$$Directivity \approx 10 \text{Log} \left( \frac{35230}{HPBW_E^\circ \times HPBW_H^\circ} \right) \text{ dB} \quad (1)$$

In this equation,  $HPBW_E$  and  $HPBW_H$  are, respectively, the half-power beamwidths of the antenna on the E- and H-planes. Given that the antenna directivity is related to the

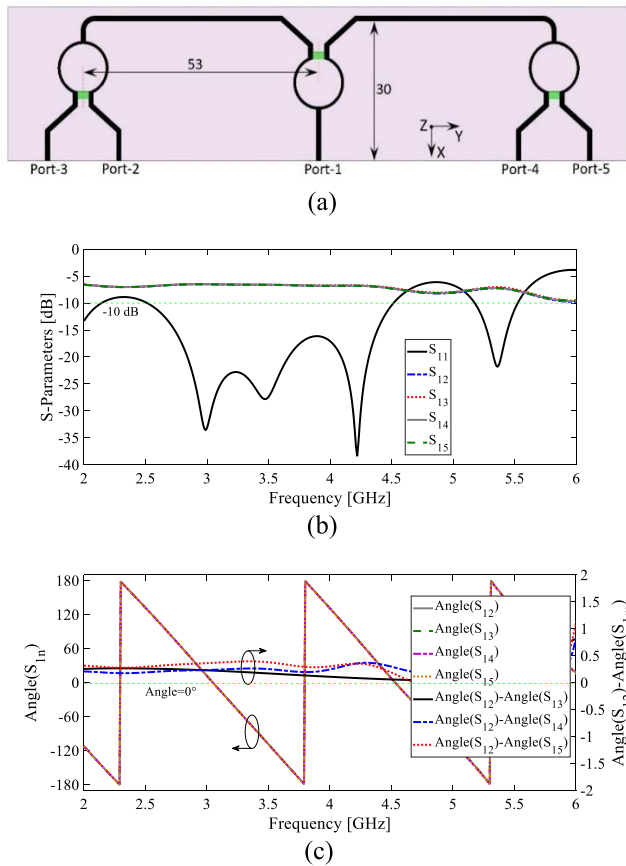


**FIGURE 7.** Proposed feeding network and simulation results (a) dimensions and configuration of the proposed feeding network, (b) S-parameters of the feeding network, and (c) phase responses of the feeding network.

inverse of the beamwidth, providing an array structure and reducing the beamwidth on the H-plane can almost double the amount of directivity and meet the needs of these systems. The array antenna structure proposed in this work is illustrated in Fig. 8.

A  $1 \times 4$  patch antenna array with a narrow radiation pattern with a beamwidth of  $21^\circ$  on the H-plane is introduced. The proposed structure is composed of two substrates. In the lower substrate, the feeding network, and in the upper substrate, the radiation elements of the array antenna are located. In the middle layer between the two substrates, the ground plane is positioned, and the microstrip lines related to the feeding network and the antenna elements are isolated. In this design, four feeding pins connect the network outputs to the radiation elements through four holes on the ground plane and transmit the signal in vertical currents to the radiation patches. The simulation and experimental results of the return loss response of the proposed array antenna are shown in Fig. 9. The simulation indicates that the array antenna has an operating frequency range of 3.34-3.73GHz (11.03%), and according to the measured result, the operating frequency band is 3.38-3.76 GHz (10.64%).

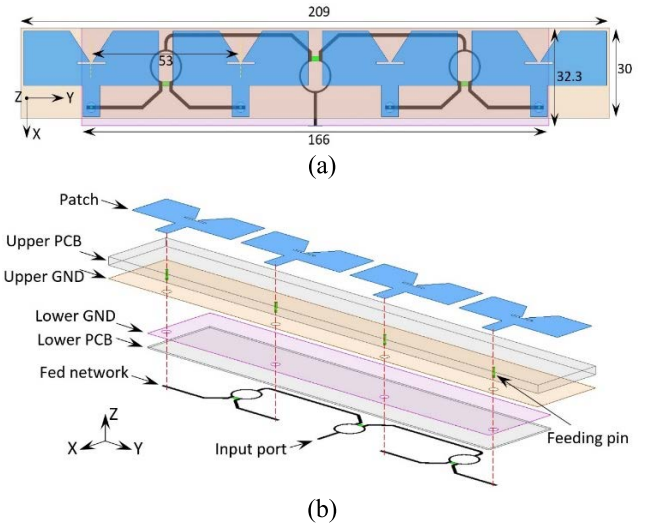


**FIGURE 8.** Proposed patch antenna array configuration (a) dimensions of the proposed patch antenna array at the front-view, and (b) 3D view of the layers of the proposed patch antenna array. Simulated and measured S11 responses of the patch antenna array.

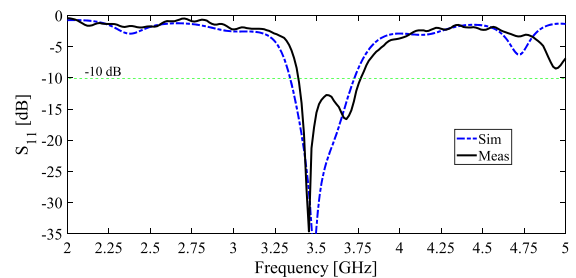


**FIGURE 9.** Simulated and measured S11 responses of the patch antenna array.

The measured and simulated results of the radiation pattern on two panels, E and H, are demonstrated in Fig. 10. It can be seen that the array antenna has a beamwidth of  $94.2^\circ$  on the E-plane and  $21.2^\circ$  beamwidth on the H-plane. Radiation patterns are relatively stable, and the difference between the Co- and Cross-polarization levels at 3.5 GHz is more than 25 dB.

The gain of the array antenna is shown in Fig. 11. According to the simulation result, the array antenna has a maximum gain of 9.83 dB, and the maximum measured gain is 9.73 dB both of them at 3.5 GHz. All the simulations are carried out using a full-wave EM simulator HFSS in this study. The slight difference between the experiments and the simulations in this design can be associated with the measurement error and the low accuracy of placing the upper and lower substrates on top of each other.

### V. MODIFIED ANTENNA ARRAY WITH A REFLECTOR PLANE

In the design of the array antenna in the previous section, due to the presence of the feeding network in the lower layer of the

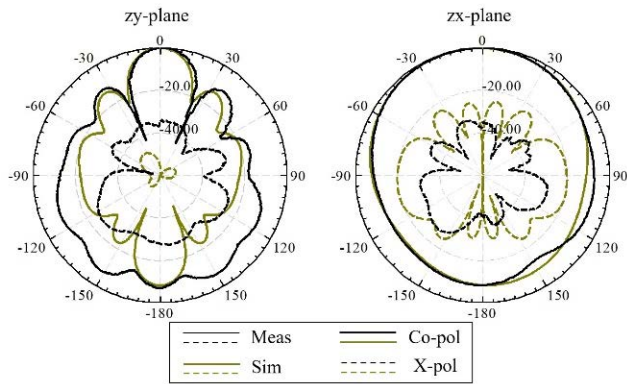


FIGURE 10. The radiation pattern of the patch antenna array.

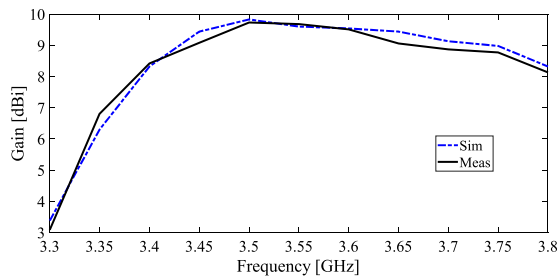


FIGURE 11. Simulated and measured gains of the patch antenna array.

antenna, the level of the back radiation is significant. In this section, to improve the radiation behavior of the antenna and reduce the back radiation level, a conductor plane is used as a reflector under the antenna. In addition to reflecting the radiation pattern upwards, this conductor plane also reduces the destructive effect of unwanted radiation from the feeding network. The final structure of the proposed array antenna with the reflector plane underneath the feeding network is shown in Fig. 12. According to this figure, two plastic spacers with the dimension of  $30 \times 3 \text{ mm}^2$  and thickness of  $\lambda/4$  ( $\lambda$  is the free space wavelength at the center frequency of the antenna operating bandwidth) are used to support the reflector plane under the antenna.

The simulated and measured results of the return loss response of the proposed array antenna with the reflector plane are presented in Fig. 13. The experiment indicates that the array antenna has an operating frequency band of 3.35-3.75 GHz (11.27%).

The measured and simulated E- and H-plane radiation patterns are illustrated in Fig. 14. It is observed that the array antenna with the reflector plane has a beamwidth of  $85.44^\circ$  on the E-plane and  $23.86^\circ$  beamwidth on the H-plane. Compared to the previous section, the radiation pattern of the final proposed patch antenna array with the reflector plane has been improved and the back radiation has been reduced by about two times.

The simulated and measured gains of the array antenna with the reflector plane are exposed in Fig. 15. It is observed

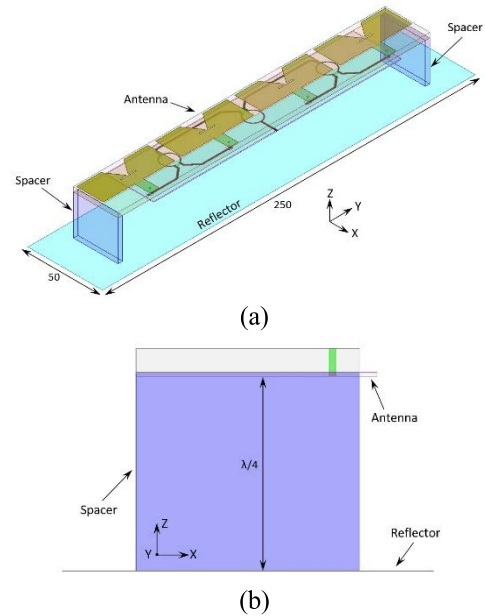


FIGURE 12. The final structure of the proposed patch antenna array with the reflector plane (a) 3D-view, and (b) side-view.

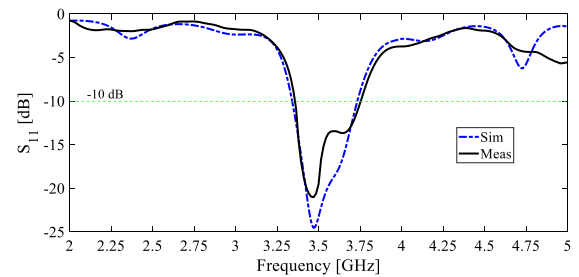


FIGURE 13. Simulated and measured S11 responses of the final proposed patch antenna array with the reflector plane.

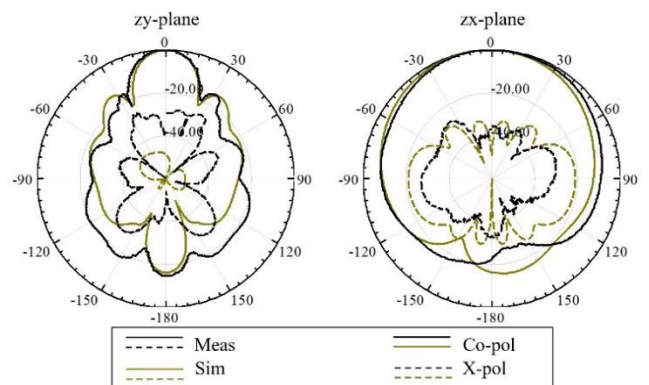


FIGURE 14. The radiation pattern of the final proposed patch antenna array with the reflector plane.

that the proposed final array antenna has a maximum gain of 10.91 dB, which has increased by 12.13% compared to the previous section. The antenna gain diagrams in this work,

TABLE 1. Comparison of the proposed patch antenna array with other fan-beam antennas.

Ref.	Operating Frequency [GHz]	Peak Gain [dBi]	HPBW <sub>E</sub> & HPBW <sub>H</sub> [°]	Size	Antenna type	Application	Element number
[4]	186	34	18 & 0.4	$371.98\lambda_0 \times 309.98\lambda_0 \times 31\lambda_0$	Pillbox	Imaging system	1
[6]	23.7	11.1	150 & 10	$5.75\lambda_0 \times 2.96\lambda_0 \times 0.13\lambda_0$	Patch	Automotive radar	8
[7]	3.3 & 3.5	11	79 & 26	$1.92\lambda_0 \times 0.35\lambda_0 \times 0.41\lambda_0$	GCPW	Radar	4
[8]	5.5	12	59 & 17	$5.15\lambda_s \times 1.66\lambda_s \times 0.27\lambda_s$	NB-CSRR	Radar	8
[11]	28	11.16	256.72 & –	$28.85\lambda_s \times 13.46\lambda_s \times 0.04\lambda_s$	Quasi-Yagi	5G	8
[13]	5.8	3.99	168 & 85	$0.60\lambda_0 \times 0.32\lambda_0 \times 0.03\lambda_0$	Dipole	ISM	1
[17]	10.4	18.2	60 & 10	$10.87\lambda_s \times 9.66\lambda_s \times 0.09\lambda_s$	Metasurface lens	Back-haul	18×16
[18]	5.5	17.5	– & 10.4	$10.98\lambda_s \times 2.60\lambda_s \times 0.26\lambda_s$	Dipole	IEEE 802.11ac	10
<b>This work</b>	3.5	10.91	85.4 & 23.8	$4.59\lambda_s \times 0.71\lambda_s \times 0.08\lambda_s$	Patch	Radar & 5G	4

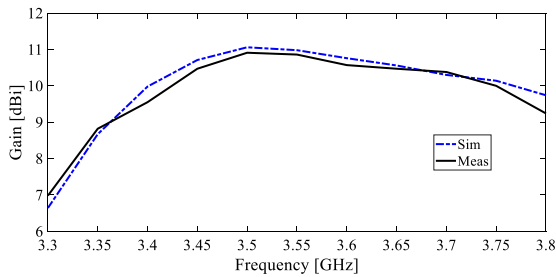


FIGURE 15. Simulated and measured peak gains of the patch antenna array with the reflector plane.

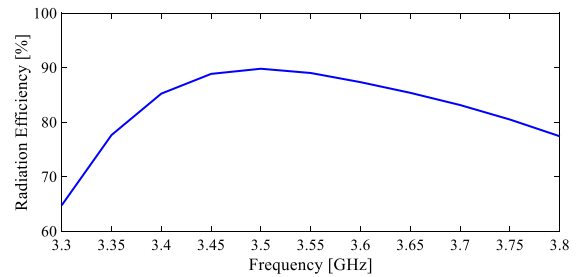


FIGURE 17. Simulated radiation efficiency of the patch antenna array with the reflector plane.

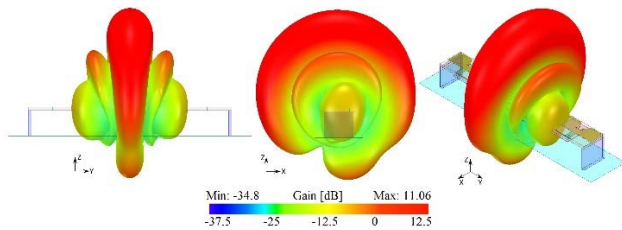


FIGURE 16. Simulated 3D radiation pattern of the patch antenna array with the reflector plane.

have been extracted in the direction of its maximum radiation ( $\varphi = 0^\circ$ , and  $\theta = 0^\circ$ ).

Correspondingly, to make a better understanding of the antenna radiation pattern, a three-dimensional representation of it is shown in Fig. 16.

Due to the radiation pattern of the array antenna, a decrease is seen in the antenna beamwidth compared to the patch antenna in Section II, which leads to an increase in the antenna gain in the array configuration. Furthermore the simulated radiation efficiency of the patch antenna array with the reflector plane is plotted in Fig. 17. The proposed antenna has a peak radiation efficiency of 89.8% at 3.5 GHz frequency.

Photos of the fabricated proposed antennas and the antenna test steps in the anechoic chamber are shown in Fig. 18. In this study, an Agilent E8363C Network Analyzer was used to test the proposed antennas.

Table 1 compares the performance of the proposed array antenna with other fan-beam antennas. It can be seen that the proposed array antenna has the merit of compactness due to the operating frequency and realized gain.

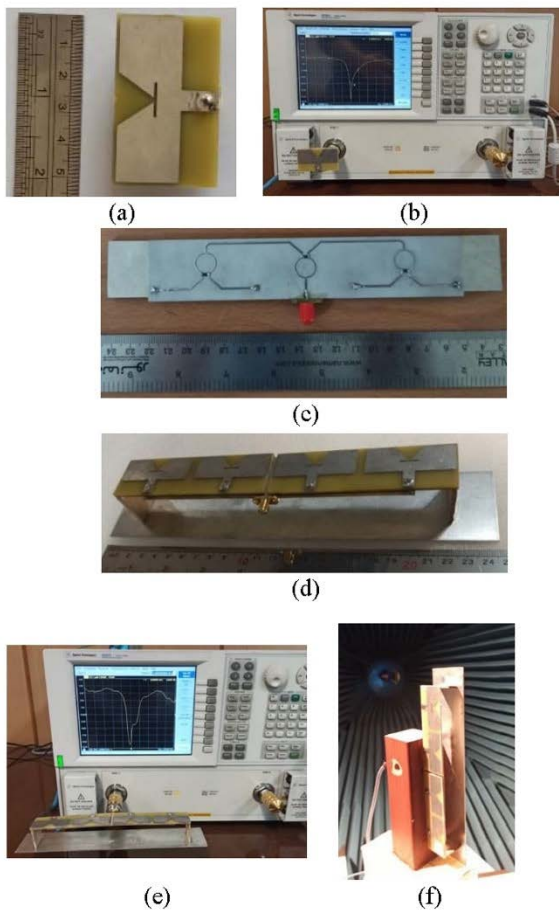


**FIGURE 18.** (a) Fabricated proposed patch antenna, (b) patch antenna connected to the VNA, (c) the feed network of the proposed array antenna, (d) 3D view of the fabricated proposed array antenna with the reflector plane, (e) antenna connected to the VNA, and (f) antenna in the anechoic chamber.

## VI. CONCLUSION

A high-gain and compact size fan-beam array antenna for radar applications and 5G systems is presented in this paper. The measurement results approve that the proposed array antenna has a wide impedance bandwidth of 3.35-3.75 GHz (11.27%), HPBW of 85.4°, and 23.8° on the E- and H-planes and a maximum gain of 10.91 dB. These results are achieved while the proposed array antenna with a two-layer structure has small dimensions of  $209 \times 32.3 \times 3.708 \text{ mm}^3$  and has smaller dimensions compared to similar fan-beam antennas. Furthermore applying a reflector underneath the antenna decrease the antenna back radiation by about two times and is improved the radiation pattern.

## REFERENCES

- [1] Z. Chen, *Handbook of Antenna Technologies*. Singapore: Springer, 2020.
- [2] Y. Huang and K. Boyler, *Antennas: From theory to Practice*. Chichester, U.K.: Wiley, 2008.
- [3] S. Gu, C. Li, X. Gao, Z. Sun, and G. Fang, "Terahertz aperture synthesized imaging with fan-beam scanning for personnel screening," *IEEE Trans. Microw. Theory Techn.*, vol. 60, no. 12, pp. 3877–3885, Dec. 2012.
- [4] S. G. Hay, J. W. Archer, G. P. Timms, and S. L. Smith, "A beam-scanning dual-polarized fan-beam antenna suitable for millimeter wavelengths," *IEEE Trans. Antennas Propag.*, vol. 53, no. 8, pp. 2516–2524, Aug. 2005.
- [5] Y.-J. Park and W. Wiesbeck, "Offset cylindrical reflector antenna fed by a parallel-plate Luneburg lens for automotive radar applications in millimeter-wave," *IEEE Trans. Antennas Propag.*, vol. 51, no. 9, pp. 2481–2483, Sep. 2003.
- [6] C.-A. Yu, E. S. Li, H. Jin, Y. Cao, G.-R. Su, W. Che, and K.-S. Chin, "24 GHz horizontally polarized automotive antenna arrays with wide fan beam and high gain," *IEEE Trans. Antennas Propag.*, vol. 67, no. 2, pp. 892–904, Feb. 2019.
- [7] M. Rahman, M. NaghshvarianJahromi, S. Mirjavadi, and A. Hamouda, "Bandwidth enhancement and frequency scanning array antenna using novel UWB filter integration technique for OFDM UWB radar applications in wireless vital signs monitoring," *Sensors*, vol. 18, no. 9, p. 3155, Sep. 2018.
- [8] P. Aguila, G. Zamora, F. Paredes, F. Martin, and J. Bonache, "Planar fan-beam reflective array antenna based on non-bianisotropic complementary split-ring resonators (NB-CSRRs)," in *Proc. IEEE Int. Symp. Antennas Propag. USNC/URSI Nat. Radio Sci. Meeting*, Jul. 2017, pp. 1263–1264.
- [9] Y.-L. Lyu, X.-X. Liu, P.-Y. Wang, D. Erni, Q. Wu, C. Wang, N.-Y. Kim, and F.-Y. Meng, "Leaky-wave antennas based on noncutoff substrate integrated waveguide supporting beam scanning from backward to forward," *IEEE Trans. Antennas Propag.*, vol. 64, no. 6, pp. 2155–2164, Jun. 2016.
- [10] M. A. Saada, T. Skaik, and R. Alhalabi, "Design of efficient microstrip linear antenna array for 5G communications systems," in *Proc. Int. Conf. Promising Electron. Technol. (ICPET)*, Oct. 2017, pp. 43–47.
- [11] S. Kim and J. Choi, "Quasi-yagi slotted array antenna with fan-beam characteristics for 28 GHz 5G mobile terminals," *Appl. Sci.*, vol. 10, no. 21, p. 7686, Oct. 2020.
- [12] W. El-Halwagy, R. Mirzavand, J. Melzer, M. Hossain, and P. Mousavi, "Fence shaping of substrate integrated fan-beam electric dipole for high-band 5G," *Electronics*, vol. 8, no. 5, p. 545, May 2019.
- [13] M. Ye, X.-R. Li, and Q.-X. Chu, "Single-layer circularly polarized antenna with fan-beam endfire radiation," *IEEE Antennas Wireless Propag. Lett.*, vol. 16, pp. 20–23, 2017.
- [14] S. Maddio, "A novel circularly polarized fan-beam antenna for 5.8 GHz DSRC applications," *Prog. Electromagn. Res. M*, vol. 98, pp. 55–65, 2020.
- [15] Y.-C. Chen, C.-K. Wu, and C. K. C. Tzuang, "Dual-frequency electric-magnetic-electric microstrip leaky-mode antenna of a single fan beam," *IEEE Trans. Microw. Theory Techn.*, vol. 50, no. 12, pp. 2713–2720, Dec. 2002.
- [16] M. R. Rahimi, N. Bayat-Makou, and A. A. Kishk, "Millimeter-wave substrate integrated gap waveguide leaky-wave antenna for WiGig applications," *IEEE Trans. Antennas Propag.*, vol. 67, no. 9, pp. 5790–5800, Sep. 2019.
- [17] H. Wang, X. Dong, J. Shen, S. Zhou, H. Wang, and Z. Wang, "Fan-beam antenna design based on metasurface lenses," *Int. J. RF Microw. Comput.-Aided Eng.*, vol. 31, no. 4, Apr. 2021.
- [18] T. T. Toan, N. M. Tran, and T. Vu Bang Giang, "A low sidelobe fan-beam series fed linear antenna array for IEEE 802.11 ac outdoor applications," in *Proc. Int. Conf. Adv. Technol. Commun. (ATC)*, Oct. 2017, pp. 161–165.
- [19] K. K. Katare, A. Biswas, and M. J. Akhtar, "Wideband beam-steerable configuration of metasurface loaded slot antenna," *Int. J. RF Microw. Comput.-Aided Eng.*, vol. 28, no. 8, Oct. 2018, Art. no. e21408.
- [20] J. Bang and J. Choi, "A compact hemispherical beam-coverage phased array antenna unit for 5G mm-wave applications," *IEEE Access*, vol. 8, pp. 139715–139726, 2020.
- [21] G. Sharifi, Y. Zehforoosh, T. Sedghi, and M. Takrimi, "Circularly polarized beam steering array antenna fed by low magnitude and phase error response of Butler matrix to use pattern stabilization applications," *Int. J. RF Microw. Comput.-Aided Eng.*, vol. 32, no. 3, Mar. 2021, Art. no. e23022.
- [22] G. Sharifi, Y. Zehforoosh, T. Sedghi, and M. Takrimi, "A high gain pattern stabilized array antenna fed by modified Butler matrix for 5G applications," *AEU Int. J. Electron. Commun.*, vol. 122, Jul. 2020, Art. no. 153237.
- [23] W. L. Stutzman, "Estimating directivity and gain of antennas," *IEEE Antennas Propag. Mag.*, vol. 40, no. 4, pp. 7–11, Aug. 1998.



**SEYED HOJATOLLAH MADANI** was born in Naghadeh, Iran, in 1982. He received the M.S. degree in telecommunication engineering from Islamic Azad University, Urmia, Iran, in 2015, where he is currently pursuing the Ph.D. degree in electrical and telecommunications. His current research interest includes patch antenna array with fan-beam characteristics.



**TOHID SEDGHI** received the B.S. degree in electronic engineering from the Department of Electrical Engineering, Islamic Azad University, Urmia Branch, Urmia, Iran, in 2007, the M.S. degree in electrical engineering from the University of Urmia, Urmia, in 2009, and the Ph.D. degree from the Department of Electrical Engineering, Science and Research Branch, Islamic Azad University, Tehran, Iran, in 2015. He is currently an Assistant Professor at the Department of Electrical Engineering, Islamic Azad University, Urmia Branch. He has published more than 30 papers in his refereed international journal and more than 15 papers in national/international conferences. His research interests include antennas and propagation, radar application, intelligent computing, and data compression.

...



**YASHAR ZEHFOROOSH** was born in Urmia, Iran, in 1981. He received the M.S. degree from Urmia University, Urmia, in 2007, and the Ph.D. degree in telecommunication engineering from the Science and Research Branch, Islamic Azad University, Tehran, Iran, in 2012. He is currently an Associate Professor with the Department of Electrical Engineering, Islamic Azad University, Urmia Branch, Urmia. He is also the Head of the Microwave and Antenna Research Center, Islamic

Azad University, Urmia Branch. His current research interests include microwave, electromagnetic components, MIMO systems, and antennas.